ELSEVIER

Cement & Concrete Composites 24 (2002) 101–117

Cement & Concrete Composites

www.elsevier.com/locate/cemconcomp

Corrosion prevention and remediation strategies for reinforced concrete coastal bridges

S.D. Cramer [a,*], B.S. Covino Jr. [a], S.J. Bullard [a], G.R. Holcomb [a], J.H. Russell [a], F.J. Nelson [b], H.M. Laylor [b], S.M. Soltesz [b]

[a] *Albany Research Center, US Department of Energy, 1450 Queen Avenue S.W., Albany, OR 97321, USA*
[b] *Oregon Department of Transportation, 200 Hawthorne Street S.E., Suite B-240, Salem, OR 97310, USA*

Abstract

Oregon's coastal highway includes over 120 bridges, most of which are reinforced concrete bridges. Twelve are historic structures. Over 40,000 m^2 of bridge surface has been repaired and is protected from further corrosion damage using thermal-sprayed zinc anodes in impressed current and galvanic cathodic protection (CP) systems. In addition, thermal-sprayed titanium, thermal-sprayed Al–12Zn–0.2In, and zinc-hydrogel anodes are being evaluated in demonstration projects on coastal bridges. Thermal-sprayed zinc anodes are estimated to have a service life exceeding 25 yr but exhibit increasing anode polarization with electrochemical age. Humectants such as lithium nitrate and lithium bromide can reduce anode polarization and extend anode service life. Catalyzed thermal-sprayed titanium anodes develop no significant anode polarization and exhibit stable long-term performance. Zinc-hydrogel galvanic anodes produce a stable protection current with no evidence of aging effects. One of the more powerful and economical tools available for assessing potential corrosion problems in a structure and for characterizing the corrosivity of bridge microclimates is chloride profiling. Current Oregon DOT specifications call for the use of stainless steel reinforcing bar in deck, beams, and precast prestressed girders, and of microsilica concrete in all future coastal bridge construction. Stainless steel bar adds a 10% premium to total project cost compared to black iron bar but is expected to reduce cumulative costs by 50% over the 120+ yr bridge life.

Keywords: Reinforced concrete; Cathodic protection; Anodes; Electrochemical aging; Microsilica concrete; Reinforcing bar; Chloride; Zinc; Titanium; Zinc-hydrogel; Stainless steel; Forensic analysis; Bridge failures

1. Introduction

Bridges located in coastal environments and in colder climates where they are exposed to repeated applications of deicing salts suffer many of the same corrosion problems. Salt contamination of concrete causes corrosion of the embedded steel reinforcement. This leads to cracking of the concrete from the expansive forces of the corrosion product. Bridges must eventually be repaired, rehabilitated, or replaced when this occurs.

A 1993 report to the Federal government stated that 44% of the more than 500,000 bridges in the US were either structurally deficient or should be posted for weight restrictions [1]. Costs for bridge maintenance, rehabilitation, and replacement due to corrosion damage are a necessary but nonproductive use of Department of Transportation (DOT) resources. Safety concerns, disruptions in service, and economic impacts of catastrophic bridge failures are further liabilities for bridge owners and users. Better construction and rehabilitation practices that mitigate these costs and liabilities require understanding the causes of corrosion-related bridge failures, and the complex interplay between the physical, chemical, and mechanical properties of concrete and steel reinforcing bar. Technology is needed to prevent further corrosion damage to existing bridges and to yield a 120+ yr bridge service life in new construction. The present paper summarizes joint research by the Albany Research Center, US Department of Energy, and the Oregon DOT to address these issues for reinforced concrete bridges, with the primary focus on planar anodes for bridge cathodic

* Corresponding author. Fax: +1-541-967-5914.
E-mail address: cramer@alrc.doe.gov (S.D. Cramer).

0958-9465/02/$ - see front matter
PII: S0958-9465(01)00031-2

protection (CP) systems, bridge construction practices and evaluation methodology, and stainless steel applications in new bridge construction.

2. Cathodic protection of historic bridges

The Oregon coast is graced by 12 irreplaceable steel-reinforced concrete bridges designed and built by respected bridge Engineer Conde B. McCullough in the 1930s. In addition, the Oregon DOT maintains more than 120 coastal bridges, most of which are reinforced concrete structures over 15 m (50 ft) in length. A 1984 report by Oregon DOT [2] raised concerns about the ongoing deterioration of these bridges, rising maintenance and repair costs, and the need to protect Oregon's large investment in coastal bridges. The worst concerns of the report were realized in 1988 with replacement of the historic 900 m (3011 ft) Alsea Bay Bridge at a cost of about $45,000,000 US (1988 dollars).

Cathodic protection is one of the most effective techniques for controlling corrosion damage in existing reinforced concrete bridges [3]. More than 500 bridges in North America are currently protected by CP systems [4]. Current distribution to the reinforcing bar is a critical factor in the design and effectiveness of these systems. The California Department of Transportation (CALTRANS) pioneered the use of planar consumable thermal-sprayed zinc anodes for optimum current distribution in a CP system installed on the Richmond-San Rafael Bridge (California, USA) in 1983 [5]. Since 1988, the Oregon DOT has installed impressed current thermal-sprayed zinc anode CP systems on five bridges: Cape Creek, Yaquina Bay, Depoe Bay, Big Creek, and Cape Perpetua. Total installed capacity of these systems exceeds $40,000\ m^2$ ($420,000\ ft^2$), with an average cost for the systems of $\$151.50\ US/m^2$ ($\$14.09\ US/ft^2$) (1997 dollars). Fifty percent of this cost is for installation of the thermal-sprayed zinc anode, the remainder for bridge rehabilitation [6]. Oregon DOT currently plans installation of thermal-sprayed zinc anode CP systems on the Rogue River, Ben Jones, and Cummins Creek bridges.

In addition to thermal-sprayed zinc anodes, a demonstration project for non-consumable thermal-sprayed titanium anodes is being conducted on the Depoe Bay Bridge [7,8]. Other demonstration projects include thermal-sprayed Al–12Zn–0.2In and zinc-hydrogel anodes on the Cape Perpetua Bridge [9,10].

Field and laboratory research has been conducted to identify characteristics of electrochemically aged planar anodes that could affect their long-term performance in bridge CP systems. Of particular interest were anode bond strength, durability, and polarization, and the impact of coastal environments on these properties. Demonstration projects are being conducted to assess the suitability of planar anodes for large-scale CP systems.

3. Field and laboratory anode aging studies

Laboratory anode electrochemical aging studies used cast concrete slabs measuring $23 \times 33 \times 5\ cm^3$ ($9 \times 13 \times 2\ in.^3$) and contained expanded steel mesh for the cathode at a cover depth of 3.2 cm (1.25 in.) to simulate bridge structural elements. The concrete mix approximated that used in Oregon's coastal bridges in the 1930s and had a water–cement (w/c) ratio of 0.48. Sodium chloride was added to the concrete at a concentration of 3 kg $NaCl/m^3$ (5 lb $NaCl/yd^3$) of concrete to approximate the present salt content in older bridges at the level of the reinforcing bar. The slabs were cured 28 days in a moist room and air dried about one month. The top face of each slab was lightly sandblasted to remove laitance and yield a medium sandpaper texture with some aggregate exposed.

Anodes were applied to the slab top face either by the twin-wire arc-spray (thermal-spray) process or, in the case of zinc-hydrogel, by affixing the conductive adhesive back of the zinc foil to the concrete and pressing the anode into the concrete with a hard roller. In each case, the nominal anode to cathode area ratio was 1:1. Twin-wire arc-spray parameters are included in Table 1 for several anode materials [11]. The 3.2 and 4.7 mm (1/8 and 3/16 in.) diameter wires are available in solid and cored versions to increase the variety of materials that can be sprayed. Thermal-sprayed anodes for laboratory studies were prepared using robotic control, an XY spray pattern, and multiple spray passes to build up an anode of uniform thickness.

Anode electrochemical age is the cumulative charge that crosses the anode–concrete interface (as the result of the anode reaction) per unit area. The anode aging rate is directly proportional to the anode current density. Laboratory impressed current CP (ICCP) aging studies were conducted at accelerated rates, compared to the current density ($2.2\ mA/m^2$ ($0.2\ mA/ft^2$)) Oregon DOT uses on coastal bridges, to determine performance characteristics that develop with anode aging and to identify worst-case problems. Galvanic CP (GCP) studies were conducted at a rate determined by a shunt resistor that limited the voltage between the anode and steel cathode to 5 mV or less. Laboratory aging studies were conducted in low and high humidity enclosures operated at 45% relative humidity (RH) and 29°C (85°F), and 80% RH and 27°C (80°F), respectively. Slabs were wetted daily with deionized water to simulate coastal wetting by rain, fog, and dew.

Table 1
Twin-wire arc-spray parameters for metals used as anodes in reinforced concrete bridge cathodic protection systems in coastal environments[a]

Wire diameter (mm (in.))	Current (A)	Voltage (V_{dc})	Spray rate (kg/h)	Deposition efficiency (%)
Zinc wire				
3.2 (1/8)	350	27	37.6	58.0
3.2 (1/8)	450	27	46.2	53.6
4.8 (3/16)	350	27	51.2	64.8
4.8 (3/16)	450	27	61.2	67.4
Al and Al–12Zn–0.2In wire				
3.2 (1/8)	350	32	10.3	66.3
3.2 (1/8)	450	32	13.0	62.0
4.8 (3/16)	350	32	15.9	68.9
4.8 (3/16)	450	32	17.3	77.1
Titanium wire				
3.2 (1/8)	300	36–40	Not measured	66.0

[a] Atomizing gas, air (air or nitrogen for Ti); atomizing gas pressure, 0.62–0.79 MPa (90–110 psi); spray orientation, normal to surface at 15–23 cm (6–9 in.) distance; multiple spray passes to build up anode thickness.

Anode performance in the field and laboratory studies was characterized by techniques related to the practical aspects of anode operation. Anode polarization was characterized by the ICCP system circuit resistance, i.e., the voltage between anode and reinforcing bar divided by current density. Concentration polarization of the anode and electrolyte (concrete) resistance, including resistance from minerals formed at the anode–concrete interface from anode dissolution products, were the major sources of system circuit resistance. Anode activation polarization, which is typically on the order of several tenths of a volt [12], is a relatively small source of circuit resistance.

Anode bond strength measurements related changes in anode–concrete interface chemistry to the mechanical durability of the anode. Anode resistivity measurements tracked composition changes within the anode. Interfacial pH measurements related anode reaction products to mineral stability fields in potential–pH diagrams and to acidification of the interface. Anode–concrete interface cross-sections, examined by analytical scanning electron microscopy (ASEM) and X-ray diffraction (XRD), were used to quantify interface chemistry and the distribution of anode reaction products in the cement paste.

Results from the field and laboratory studies guide Oregon DOT's use of planar anodes in current and future coastal CP applications. Recommendations and results include anode installation specifications, anode consumption rates, modifications to anode operation, models for anode performance, and estimates of anode service life.

3.1. Thermal-sprayed planar zinc anodes

Thermal-sprayed planar zinc anodes for ICCP have been installed on five Oregon coastal bridges. Field and laboratory anodes were applied to lightly sand blasted concrete using the twin-wire arc-spray process and 3.2 mm (1/8 in.) diameter zinc wire [13–17]. Zinc thermal-spray parameters are given in Table 1. The zinc anode was 250–500 μm (10–20 mil) thick.

The zinc anode is a consumable anode and the anode reaction is:

$$Zn + 2H_2O \rightarrow Zn(OH)_2 + 2H^+ + 2e^- \quad (1)$$

Acidification of the anode–concrete interface occurs with aging as a result of Reaction 1. Under drying conditions dehydration of the zinc hydroxide may take place:

$$Zn(OH)_2 \rightarrow ZnO + H_2O \quad (2)$$

At the reinforcing bar, the cathode reaction is:

$$O_2 + 2H_2O + 4e^- \rightarrow 4OH^- \quad (3)$$

In laboratory studies, anodes were aged up to 2 yr at a 15-fold accelerated rate of 32.2 mA/m^2 (3 mA/ft^2) to a maximum charge of 1850 kC/m^2, equivalent to about 27 yr service at Oregon DOT bridge ICCP conditions.

Microanalysis showed the zinc anode had a porous structure comprised of moderately well-bonded thin zinc "splats". Anode resistivity ranged from 21 μΩ cm (unaged) to 43 μΩ cm (aged 1640 kC/m^2). Anode bond strength ranged from 4.0 (unaged) to 0.12 MPa (aged 1640 kC/m^2). Anode color was silver-gray.

Bond strength of periodically wetted thermal-sprayed zinc anodes varied with electrochemical age, Fig. 1. The initial bond to the concrete was mechanical involving the penetration of zinc into the concrete surface roughness. The initial bond strength decrease was associated with the rapid consumption of zinc embedded in surface roughness. Following this, the bond strength increased, because of continued curing of the concrete slabs [18] and secondary mineralization of zinc dissolution products at the anode–concrete interface. With longer aging, the

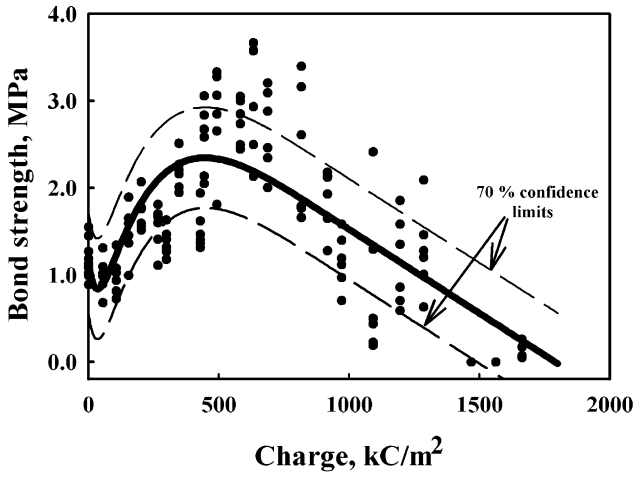

Fig. 1. Bond strength of periodically wetted thermal-sprayed zinc anodes on concrete in ICCP service as a function of electrochemical age in laboratory studies.

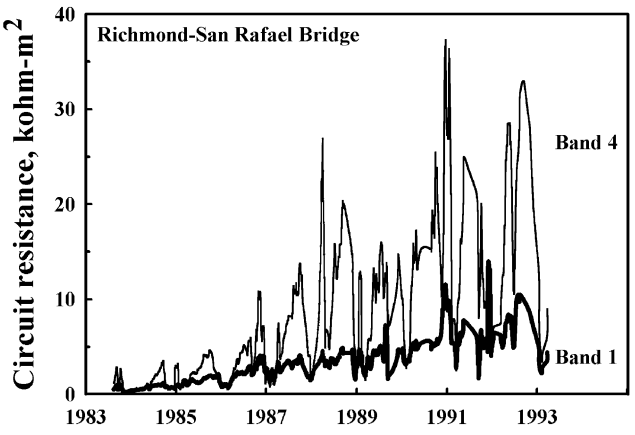

Fig. 2. Circuit resistance for thermal-spayed zinc anodes in bands 1and 4 on the Richmond-San Rafael Bridge (CA) for 10 yr of ICCP service.

bond strength decreased due to the formation of a weak zinc mineral layer at the anode–concrete interface. Based on Fig. 1, the anode service life (ending when the bond strength reached zero) was estimated to be more than 25 yr (1 yr = 69.4 kC/m^2) at the Oregon DOT coastal bridge CP current density, 2.2 mA/m^2 (0.2 mA/ft^2). Preheating of the concrete prior to anode application can boost the initial bond strength but does not materially improve the long-term anode bond strength. The bond strength decreased more rapidly when the anode was not periodically wetted. The long-term decrease in bond strength was accompanied by a decrease in anode–concrete interfacial pH from 12 to 7.

Circuit resistance remained low for laboratory aging up to about 400 kC/m^2, equivalent to about 6 yr ICCP service [13,14,17]. For longer aging, the circuit resistance (and anode polarization) increased substantially due to the formation of the same zinc mineral layer at the anode–concrete interface that caused bond strength to decrease. Circuit resistance was also particularly dependent upon patterns of anode wetting and drying.

Similar results were obtained in a field study of four thermal-sprayed zinc anode bands (zones) on the Richmond–San Rafael Bridge (California, USA) [15,17]. Zinc anode band 1 was 3.6 m above the water and exposed to precipitation and spray from waves; anode band 4 was 7.6 m above the water and sheltered by the deck. Circuit resistance of both bands increased with electrochemical age, Fig. 2, and varied seasonally with higher resistance during the dry months over the 10 yr of operation. During these dry months, circuit resistance was substantially higher for band 4, showing the effects of sheltering and distance from the water. However, the band 4 resistance approached that of band 1when both were well wetted by precipitation owing to improved ionic conductivity in the mineral layer at the anode–concrete interface.

An SEM photomicrograph of the anode–concrete interface taken from the laboratory study after electrochemical aging of 1080 kC/m^2 is shown in Fig. 3 along with K_α X-ray maps for Zn, Ca, and Cl. These figures show that: (1) the zinc anode is soluble, forming a layer of zinc minerals at the anode–concrete interface, with some dissolution of these minerals and migration of zinc ions into the concrete; (2) Ca is depleted from a reaction zone adjacent to the interface owing to acidification and to replacement by the smaller zinc ions in the cement paste; and (3) Cl ions migrate to and concentrate at the anode, leading to the formation of zinc hydroxychloride minerals at the interface.

3.2. Alternative planar anode materials

Alternative planar anode materials to the thermal-sprayed zinc anode were considered as a means for reducing ICCP circuit resistance in long-term service, increasing galvanic current output, and improving anode service life [19–21].

3.2.1. Zinc-hydrogel anode

The zinc-hydrogel anode was applied in a field trial to a 57 m^2 (614 ft^2) GCP zone on the Cape Perpetua Viaduct. Laboratory studies were also conducted using cast concrete slabs to determine anode performance during long-term ICCP and GCP aging [9,10]. The zinc-hydrogel anode is a 0.25 mm (0.010 in.) thick zinc foil, backed with a conductive, pressure-sensitive adhesive. The adhesive is a hygroscopic acrylate polymer 0.75 mm (0.030 in.) thick containing sulfonic acid. It is charged with lithium chloride to form the electrolyte. Zinc-hydrogel comes in rolls 25 cm (10 in.) wide with a removable plastic film backing to protect the adhesive.

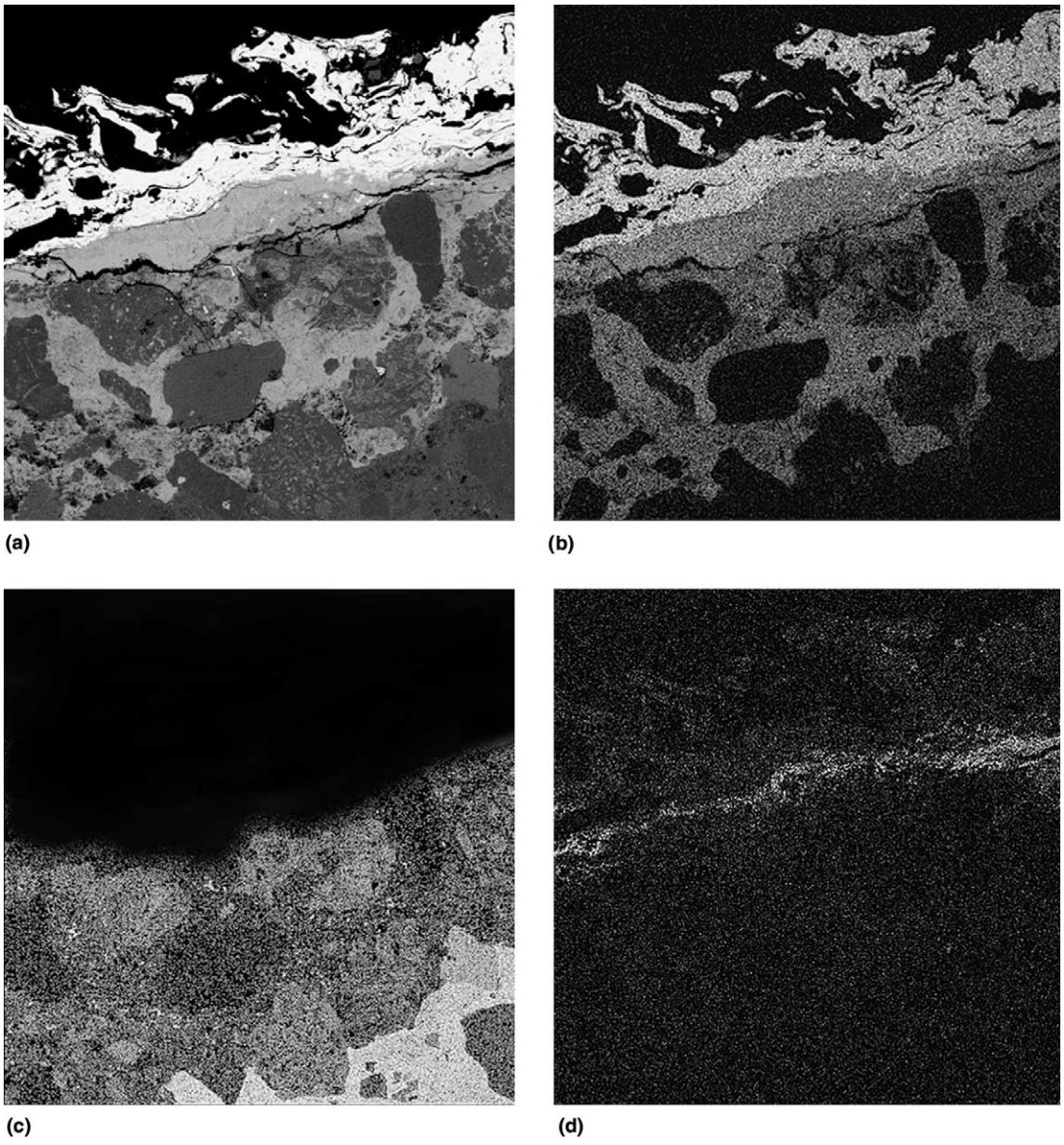

Fig. 3. SEM photomicrograph and X-ray maps of zinc anode cross-section showing anode-concrete interface after ICCP service for 1080 kC/m^2 in laboratory studies: (a) back-scattered electron SEM photomicrograph; (b) zinc X-ray map; (c) calcium X-ray map; (d) chlorine X-ray map.

Concrete preparation was the same as for thermal-sprayed zinc anode installations. The backing was peeled from the zinc foil exposing the adhesive and the foil pressed onto the concrete. With the anode applied to the concrete, the zinc was rolled with a wood or hard rubber roller to further press the adhesive into the concrete surface. The edges of the anode were sealed with silicone rubber (or polyurethane) caulking to prevent external water from reaching the adhesive and causing it to swell. The hydrogel anode color was bright silver. However, after completing a field installation, the hydrogel anode can be painted to blend with the surroundings.

The zinc-hydrogel anode is a consumable anode and the anode reaction was the same as for zinc anodes, Reaction 1. The weak sulfonic acid in the adhesive buffers the production of hydrogen ions, resulting in little change in pH at the adhesive–concrete interface. Since the adhesive is hygroscopic, conditions that could lead to dehydration of zinc hydroxide produced by the anode reaction are unlikely.

In laboratory studies, ICCP anodes were aged up to 2 yr at a 15-fold accelerated rate of 32.2 mA/m^2 (3 mA/ft^2) to a maximum charge of 1300 kC/m^2, equivalent to about 19 yr service at Oregon DOT bridge ICCP conditions. The bond strength of the zinc-hydro-

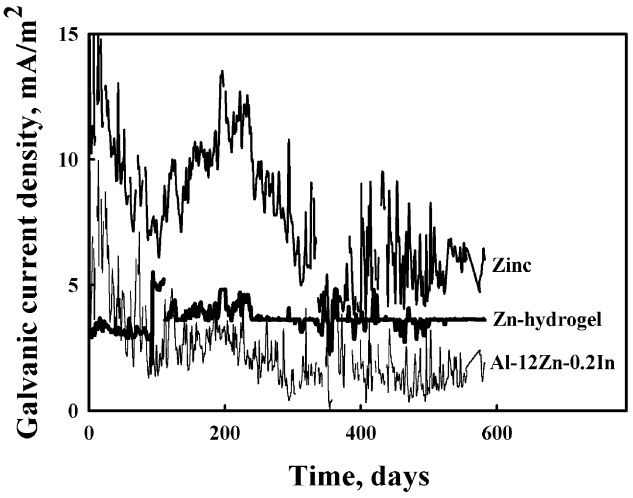

Fig. 4. Current output from galvanic zinc-hydrogel, and thermal-sprayed zinc and Al-12Zn-0.2In anodes on the Cape Perpetua Half-Viaduct (OR).

gel ranged from 0.12 MPa (unaged) to 0.01 (aged 1300 kC/m^2). While the bond strength was not initially high and decreased with age, the anode did not disbond from the concrete at any time during aging. Circuit resistance varied little with aging except when the adhesive became dry; and then it rose substantially. Analytical SEM showed that the adhesive served as a substantial sink for zinc reaction products produced by Reaction 1.

GCP anodes aged 530 days in the laboratory and 580 days on the Cape Perpetua Viaduct gave similar results. Current output from the field trial is shown in Fig. 4. The zinc-hydrogel anode current output was a steady 3.6 mA/m^2 (0.3 mA/ft^2), adequate to protect reinforcing bar at Oregon DOT coastal bridge CP conditions. In the laboratory, current output fell when the adhesive became dry, a condition that did not occur in the field trial. Zinc-hydrogel current output was much more stable with time than the output from a thermal-spray zinc anode on a neighboring 57 m^2 (614 ft^2) GCP zone on the Cape Perpetua Viaduct, Fig. 4.

3.2.2. Thermal-sprayed Al–12Zn–0.2In anode

The thermal-sprayed Al–12Zn–0.2In anode was used on a 57 m^2 (614 ft^2) GCP zone of the Cape Perpetua Viaduct. Laboratory studies were also conducted using cast concrete slabs to determine anode performance during long-term ICCP and GCP aging [9,10]. Anodes were applied to lightly sand blasted concrete using the twin-wire arc-spray process and 3.2 mm (1/8 in.) diameter cored aluminum wire. The cored aluminum wire contained a mechanically mixed Zn–In powder that yielded the Al–12Zn–0.2In composition on melting. Al–12Zn–0.2In thermal-spray parameters are essentially the same as for Al wire and are given in Table 1. Anode thickness was 180 μm (7 mil) for the laboratory study and 400 μm (15 mil) for the field trial. Analyses showed the "as-received" Al–12Zn–0.2In cored wire used in this study and the resulting anode contained 0.08% copper. Presently available wire contains less than 0.01% copper.

The Al–12Zn–0.2In anode is a consumable anode resulting in both zinc and aluminum loss during cathodic protection. The indium is added to the alloy to prevent passivation of the Al in the high pH concrete environment. The anode reactions are the dissolution reaction for zinc, Reaction 1, plus the aluminum reaction:

$$2Al + 3H_2O \rightarrow Al_2O_3 + 6H^+ + 6e^- \quad (4)$$

In addition, since concrete has a fairly high pH, Al_2O_3 may dissolve to form aluminate ions:

$$Al_2O_3 + H_2O \rightarrow 2AlO_2^- + 2H^+ \quad (5)$$

However, acidification of the anode–concrete interface by Reactions 1 and 4 would mitigate against Reaction 5. Dehydration of the zinc hydroxide, Reaction 2, may also occur.

In laboratory studies, ICCP anodes were aged up to 1 yr at 5-, 10-, and 15-fold accelerated rates. For example, at a 5-fold accelerated rate or 10.7 mA/m^2 (1 mA/ft^2), anodes were aged to a maximum charge of 263 kC/m^2, equivalent to about 3.8 yr service at Oregon DOT bridge ICCP conditions. Anode performance decreased with increase in anode current density. Anodes operated at the higher current densities (10- and 15-fold) disbonded after a charge of 140 kC/m^2, equivalent to 2.0 yr service. Bond strength decreased with electrochemical age and the decrease was more rapid for higher anode current densities. The bond strength at a 5-fold accelerated rate ranged from 3.6 (unaged) to 0.8 MPa (aged 175 kC/m^2).

Analytical SEM analysis showed that zinc dissolution products migrated into the cement paste, as was observed for thermal-sprayed zinc anodes. However, aluminum dissolution products did not migrate, but rather Al_2O_3 formed within the anode at the dissolution site. Since Al_2O_3 has a larger volume than the Al consumed, the resulting expansive forces that develop with increasing electrochemical age caused cracks to form between individual splats and grains. These forces, plus self-corrosion observed at the anode surface, caused grains to pop out of the anode surface.

GCP anodes aged 530 days in the laboratory and 580 days on the Cape Perpetua Viaduct gave similar results. Current output from the field trial is shown in Fig. 4. The anode current output decreased with time and was strongly dependent on moisture in the structure. At 580 days in the field, the Al–12Zn–0.2In anode current output was 2.1 mA/m^2(0.2 mA/ft^2), adequate to protect reinforcing bar at Oregon DOT coastal bridge CP conditions. The Al–12Zn–0.2In anode produced less

current than either the zinc-hydrogel or the thermal-sprayed zinc anode, Fig. 4.

3.2.3. Catalyzed thermal-sprayed titanium anode

A cobalt-catalyzed, non-consumable, thermal-sprayed titanium anode was applied to one ICCP zone on the Depoe Bay Bridge (Oregon, USA) in a demonstration project as an alternative to the thermal-sprayed zinc anode. The cost for installing the catalyzed titanium anode was 18 percent more than that for installing a zinc anode. Laboratory studies were also conducted to determine long-term performance and aging characteristics of the anode [7,8].

Titanium was applied to lightly sand blasted concrete using the twin-wire arc-spray process and 3.2 mm (1/8 in.) diameter, annealed grade 1 titanium wire. Laboratory anodes were applied to cast concrete slabs. Titanium thermal-spray parameters are given in Table 1. The titanium anode was 100–150 μm (4–6 mil) thick.

The titanium anode was catalyzed using a cobalt nitrate-amine complex in pH 3.47 aqueous solution. The solution contained 60 g Co/L, with Co(II) present as the nitrate and Co(III) present as an amine complex. The Co(III)/Co(II) ratio was 0.25. The catalyst was brush applied at a coverage of 0.344 L/m^2 (0.0087 gal/ft^2) with the anode polarized anodically at a current density of 11–29 mA/m^2 (1.0–2.7 mA/ft^2) during application. Polarization of the anode continued for one month to form the active catalyst, Co_3O_4, a spinel with Co(II) in the tetrahedral interstices and Co(III) in the octahedral interstices. Co_3O_4 is a p-type semiconductor and a highly active catalyst for surface reactions involving oxygen.

The catalyzed anode reaction was the production of oxygen from water. On the Oregon coast, water is delivered to the anode in the form of dew, fog, rain, and humid air. Water is essential for successful operation of the anode. In the high pH concrete, the anode reaction initially is:

$$4OH^- \rightarrow O_2 + 2H_2O + 4e^- \quad (6)$$

However, acidification of the anode–concrete interface by consumption of hydroxyl ions eventually will change the anode reaction to:

$$2H_2O \rightarrow O_2 + 4H^+ + 4e^- \quad (7)$$

ICCP anodes were aged 2 yr in the laboratory at a 10-fold accelerated rate of 21.4 mA/m^2 (2 mA/ft^2) to a charge of 1520 kC/m^2, equivalent to about 23 yr service at Oregon DOT bridge ICCP conditions.

Microanalysis showed the titanium anode had a porous, heterogeneous structure and composition strongly affected by reactions during formation between the molten titanium, the atomizing gas, and air. Cooling rates ranged from 10 to 150 K/s, well below those that would lead to amorphous crystal structures from rapid solidification. On average the anode contained 88 wt% Ti, present as α-Ti containing interstitial nitrogen, γ-TiO, and possibly TiN. Nitrogen atomization produced coatings with more uniform chemistry, less internal cracking, and lower resistivity than air atomization. Anode resistivity ranged from 2110 μΩ cm (unaged) to 8400 μΩ cm (aged 1520 kC/m^2). Anode bond strength ranged from 1.17 (unaged) to 0.29 MPa (aged 1520 kC/m^2). Anode color was gold-brown.

The catalyzed anode was insensitive to changes in relative humidity and had a stable circuit resistance for RH from 30% to 100%, Fig. 5. This indicates sufficient water was delivered to the anode from the environment at even low RH to maintain the anode reaction. Operating voltage as a function of electrochemical age was flat for the equivalent of 23 yr (1520 kC/m^2) service at Oregon DOT conditions, with no indication that the anode would not perform similarly for longer periods. Anode–concrete interfacial pH decreased from 11 to 7 with aging. Anode bond strength and durability decreased during aging as the result of acidification of the anode–concrete interface. However, no anode spalling or disbondment was observed anytime during the experiments. Field measurements after 2 yr anode operation (46 kC/m^2) gave similar potential-current operating results. No decrease in anode–concrete interfacial pH or bond strength was observed in the field.

The anode–concrete interface from the laboratory samples, after electrochemical aging 1520 kC/m^2, was examined by SEM and with K_α X-ray maps for Ti, Ca, and Co. These analyses showed that: (1) the titanium anode was insoluble; (2) Ca was depleted from a reaction zone adjacent to the interface as the result of acidification; and (3) the Co catalyst was not depleted by

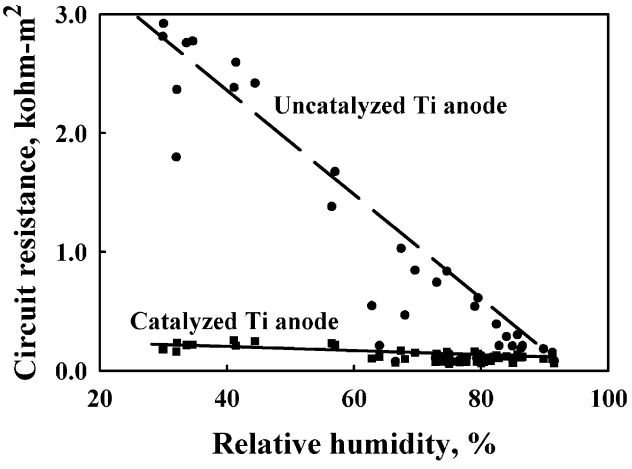

Fig. 5. Circuit resistance of catalyzed and uncatalyzed titanium anodes in ICCP service as a function of relative humidity in laboratory studies.

leaching from the concrete and was, in fact, present throughout the reaction zone. No evidence of the Ca depleted reaction zone was observed in a core sample removed from the Depoe Bay Bridge after 2 yr service (146 kC/m^2). Either it was too soon to see the effects of acidification or acidification of the anode–concrete interface was mitigated by other processes at the lower current density used by Oregon DOT.

3.3. Anode chemical treatments – humectants

Moisture substantially reduces the circuit resistance of thermal-sprayed planar zinc anode CP systems [15–17]. This reduction is associated with increasing conductivity of the electrolyte (concrete) and reducing anode concentration polarization. Humectants, salts that attract water, are one way of increasing moisture content at the anode–concrete interface. Screening studies identified two promising humectants, LiBr and $LiNO_3$ [22]. In the laboratory, these humectants were applied to unaged and previously aged thermal-sprayed zinc anodes on concrete slabs. In the field, they were applied to two thermal-sprayed zinc anode ICCP zones on the Yaquina Bay Bridge (Oregon, USA), with adjacent zones used as controls [23,24].

A saturated LiBr solution at 25°C is 16.7 *M* LiBr and is in equilibrium with air at 8% RH; for $LiNO_3$ these values are 13.0 *M* $LiNO_3$ and 45% RH [24]. However, when saturated solutions of humectants at the anode–concrete interface contact air at a higher RH, they absorb moisture from the environment to form a more dilute solution. This is the basis for the use of humectants. For example, LiBr exposed to 50% RH will absorb water until a solution of 9.0 *M* LiBr is formed; at 80% RH, a 4.0 *M* LiBr solution is formed. This raises the moisture content of the interface substantially. In doing so, it lowers local concrete resistivity (raises ionic conductivity) and improves the dispersion of zinc anode reaction products into the concrete. Furthermore, water consumed in anode Reaction 1 will be replenished by water absorbed from the environment. LiBr is the more powerful humectant at low RH, but both humectants should strongly attract moisture to the anode–concrete interface at the RH values typically found on the Oregon coast. The net effect should be to lower CP circuit resistance and lengthen zinc anode life.

In the laboratory, the effect of humectants on both new and previously aged zinc anodes was examined. Stock solutions of humectant contained 300 g humectant/L, i.e., 3.45 *M* LiBr and 4.35 *M* $LiNO_3$, and 10 ml/L of commercial surfactant to improve anode wetting. The humectants were brush applied (laboratory) or sprayed (field) on the thermal-sprayed zinc anodes at a rate of 86 g/m^2 (8.0 g/ft^2). Controls in the laboratory were treated only with the surfactant; controls in the field were two untreated thermal-sprayed zinc anode ICCP zones (Zones 10 and 14) adjacent to the treated zones (Zones 11 and 13).

The laboratory anodes were electrochemically aged in low and high humidity enclosures. ICCP experiments were aged to 400–600 kC/m^2, equivalent to 5.8 to 8.9 yr service at the rate used by Oregon DOT on coastal bridges. GCP experiments were conducted for about 2 yr.

The effect of humectants on the circuit resistance of anodes previously aged in ICCP studies is summarized in Fig. 6. The thick solid curve is the circuit resistance for untreated zinc anodes aged the equivalent of over 20 yr in 80% RH. Additional anodes were previously aged equivalent to times up to 20 yr, then treated with humectant and aged the equivalent of 5.8 to 8.9 more years. The circuit resistance of these anodes is plotted in Fig. 6 as the total electrochemical age, i.e., the sum of the previously aged period plus the additional 5.8 to 8.9 yr aging with humectant. The circuit resistance is reduced by 75% or more with the use of humectants at 80% RH. At 45% RH, the resistance was climbing but still below the curve for untreated anodes at 80% RH. $LiNO_3$ outperformed (lower circuit resistance) LiBr at both RH levels. Investigations are needed to determine whether this is due to oxidation and loss of bromide ion at the elevated anode potentials sometimes observed in these experiments.

SEM photomicrographs and K_α X-ray maps of humectant-treated zinc anodes, ICCP electrochemically aged the equivalent of 6.1 yr, showed greater dispersion of zinc into the concrete at the anode–concrete interface than would have occurred for untreated anodes. The X-ray maps showed Br concentrated in the zinc minerals

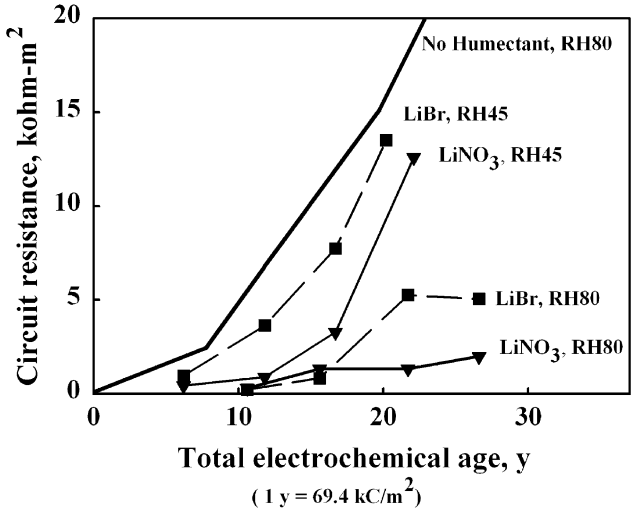

Fig. 6. Circuit resistance of pre-aged humectant-treated zinc anodes in ICCP service as a function of total electrochemical age in laboratory studies at 45% and 80% RH.

formed at the interface by aging. This suggests that LiBr (and perhaps $LiNO_3$) may be resistant to leaching from the anode by precipitation washing.

GCP current output results are shown in Fig. 7 for unaged zinc anodes in the laboratory at 80% RH. Initial current output was high for the humectant-treated anodes and the control. Current output declined and leveled out after electrochemical aging the equivalent of 0.5–1 yr. Output from the $LiNO_3$-treated zinc anode was less than from the control. The LiBr-treated zinc anode output was well above the control and leveled out to a value close to $2mA/m^2$, the level Oregon DOT uses in coastal bridge ICCP systems.

The ICCP circuit resistance for humectant treated zones on the Yaquina Bay Bridge and that of the two adjacent control zones is shown in Fig. 8. All of the

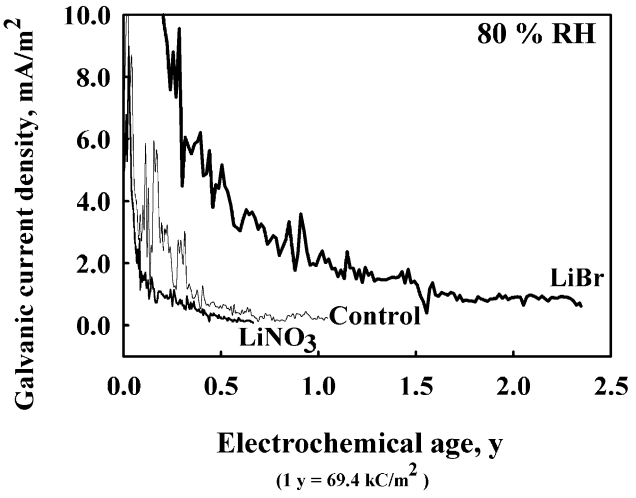

Fig. 7. Current output of galvanic humectant-treated zinc anodes in laboratory studies at 80% RH.

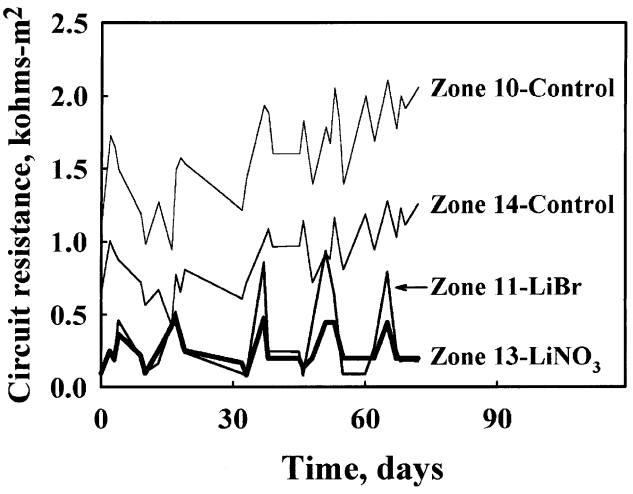

Fig. 8. Circuit resistance of controls and humectant-treated zinc anode zones in ICCP service on the Yaquina Bay Bridge (OR).

zones are over land in the approach structure to the bay crossing. Zone 10 is furthest from the bay (about 131 m [430 ft]) and Zone 14 is closest (about 73 m [240 ft]). The humectant-treated zones are physically between these two control zones at 94 m [310 ft] ($LiNO_3$) and 113 m [370 ft] (LiBr). The four zones are sheltered by the bridge deck. The higher circuit resistance of Zone 10 suggests it is the drier of the two control zones. The position of the zones relative to the bay suggests circuit resistance varies inversely with distance to the bay and that, in the absence of humectant, the circuit resistance of the Zones 11 and 13 would lie between Zones 10 and 14. Instead, humectant application substantially reduced the circuit resistance of Zones 11 and 13 compared to the controls.

Chloride profiles were measured in each of the four zones on the Yaquina Bay Bridge using the Oregon DOT powder sampling technique to characterize concrete quality and zone microclimate. This was done using Fick's second law of diffusion to compute mean surface chloride concentration, C_o, and effective chloride diffusion coefficient, D, from the chloride profiles. Fick's law parameters for the zones are given in Table 2. Diffusion coefficients were similar for each zone, indicating similar concrete quality. Surface chloride concentrations, which are determined by factors including zone microclimate (sheltering, salt deposition, dew formation, precipitation washing), decreased with distance from the bay. The driest and furthest zone from the bay, Zone 10, had the lowest value. Values increased closer to the bay where deposition from salt spray increased. However, in zone 14, precipitation washing from wind blown precipitation may also have become important and the surface chloride concentration is somewhat less than for Zone 13.

4. Bridge corrosion failures and evaluation methodology

Forensic analysis of failed coastal bridges was conducted to identify the critical factors leading to failures [25,26]. The most effective methodologies for identifying reinforcing bar corrosion problems in bridges were determined. Changes in construction practice that would prevent similar problems in new structures were identified. The results of these analyses also recognize that many advances in cement and concrete quality, and design and construction practices have occurred over the years since the failed bridges were constructed.

4.1. Rocky Point Viaduct (Oregon, USA)

The Rocky Point Viaduct (1954–1994), a five-span, 114 m (373 ft) long, reinforced concrete deck girder

Table 2
Fick's law parameters obtained by least-squares fit of chloride profile data from 40 to 60 yr old reinforced concrete bridges in coastal environments

Structure	Position on structure	Fick's law parameters[a]			
		Land face (or side)		Ocean face (or side)	
		C_o (kg Cl/m^3)	$D \times 10^8$ (cm^2/s)	C_o (kg Cl/m^3)	$D \times 10^8$ (cm^2/s)
Yaquina Bay Bridge:					
Zone 10 beam (131 m to bay)	Middle	–	–	1.67	0.595
Zone 11 beam (113 m to bay)	Middle	–	–	3.34	0.490
Zone 13 beam (94 m to bay)	Middle	–	–	6.63	0.458
Zone 14 beam (73 m to bay)	Middle	–	–	5.41	0.456
Rocky Point Viaduct:					
Beam A1, patch concrete	Low	9.62	3.14	15.00	3.25
Beam A2, original concrete	High	9.58	1.24	5.26	0.948
Brush Creek Bridge:					
Beam A2	Low	8.83	0.828	11.72	1.71
Beam A3	Low	7.05	2.44	13.14	1.53
Beam A2	High	6.29	0.799	14.76	1.38
Beam A3	High	6.91	0.799	10.08	1.90
Deck, A2	Underside	–	–	9.92	0.880
Deck, A3	Underside	–	–	7.21	0.407
Diaphragm, A2	Middle	13.43	1.08	15.41	1.56
Diaphragm, A3	Middle	9.77	1.07	17.04	0.921

[a] To convert from kg Cl/m^3 to lb Cl/yd^3 divide by 0.5932.

bridge for US Route 101 on the southern Oregon coast, was replaced in 1994 due to severe structural damage resulting from corrosion-related reinforcing bar section loss and concrete deterioration. The Viaduct was located in one of the most corrosive microclimates on the Oregon coast on an exposed headland 25 m (80 ft) from the ocean at an elevation of 35 m (115 ft).

First evidence of corrosion damage to the concrete was reported in 1967 only 13 yr after the Viaduct was constructed. A major repair of the Viaduct was conducted in 1969. The repair included removing all concrete from around reinforcing bar in the bottom of the beams and replacing it with cast patch concrete. During this repair a number of additional actions were taken to halt further corrosion damage. These included: a coal tar epoxy seal between the patch and original concrete as a barrier to chloride migration into the patch concrete; a coal tar epoxy coating on selected reinforcing bar; an inorganic zinc coating on selected reinforcing bar; and a linseed oil coating over the beam to seal the concrete from further chloride intrusion. None of these additional actions were effective and it was necessary to replace the Viaduct after only 40 yr service.

One 14 m (47 ft) beam from the Viaduct was preserved for detailed evaluation of failure causes to provide a basis for modifying repair and rehabilitation practices for existing bridges and improving construction practices for new bridges. The evaluation included: (1) the physical, mechanical and chemical properties of the Viaduct concrete; (2) a rebar corrosion damage survey; and (3) determination of the chloride distribution in the concrete and the way the chloride distribution was modified by impressed current cathodic protection.

Petrographic analysis showed that alkali-silica, alkali-carbonate, and sulfate reactions did not contribute to premature deterioration of the Viaduct. The compressive strength of the original concrete at the time of Viaduct demolition was 52.8 MPa (7.66 ksi) and continued to meet design specifications. The w/c ratio for the original concrete was 0.53. The void fraction in the original concrete was 10.6% while the patch concrete was 50 pct higher, 15.6%.

Chloride ion profiles through the full thickness of the beam from west (ocean) face to east (landward) face provided the best evidence for explaining the early failure of the Viaduct. The "as-received" profile for patch concrete is shown in Fig. 9 along with the location of shear stirrups (S) and square reinforcing bar (R). [The 0.0 yr ICCP profile in Fig. 9 is the "as-received" profile.] Profiles after 0.5 and 1.0 yr ICCP, equivalent to 5 and 10 yr service at Oregon DOT bridge CP conditions, are also included in Fig. 9. The west face of the beam was fully exposed to the ocean, sheltered only by the bridge soffit; the east (landward) face was sheltered by the deck. The "as-received" chloride profile was not symmetrical, indicating that beam microclimates and the resulting salt deposition were different on the two faces of the beam. Profiles were different for the original and the patch concrete, indicating that properties of the concrete affected chloride deposition and migration.

After 40 yr service, the shear stirrups and reinforcing bar were embedded in concrete containing chloride at

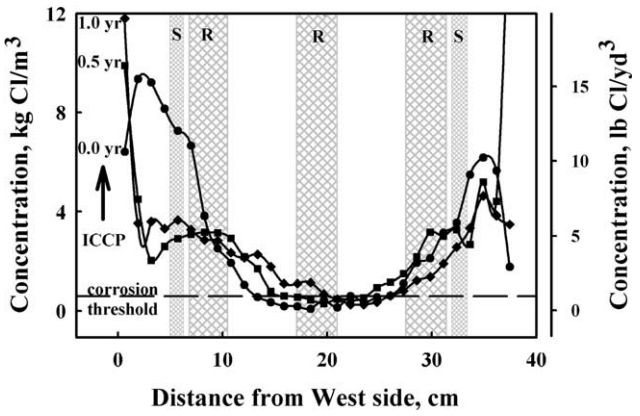

Fig. 9. Chloride profiles for 25 yr old patch concrete from the Rocky Point Viaduct (OR) as a function of thermal-sprayed zinc anode ICCP service for 0.5 and 1.0 yr. The "as-received" profile is the "0.0 yr ICCP" profile. Position of reinforcing bar (*R*) and shear stirrups (*S*), and the chloride corrosion threshold (0.74 kg Cl/m^3) are shown.

levels well above the chloride corrosion threshold for black iron bar. Numerous studies have shown the chloride corrosion threshold lies in the range 0.6–1.2 kg Cl/m^3 (1.0–2.0 lb Cl/yd^3), where the concentration is given per cubic meter (or cubic yard) of concrete [27–32]. One widely used estimate of the chloride threshold is 0.2 wt pct Cl in the cement paste [28,32], which translates into 0.74 kg Cl/m^3(1.25 lb Cl/yd^3) for the concrete described by McDonald et al. [32]. This conservative estimate of the chloride threshold was used here to illustrate the effects of chloride ion on reinforcing bar corrosion. The "as-received" curve in Fig. 9 also shows a chloride gradient between the inner and outer mats of reinforcing bar that provides the opportunity for macro-cell corrosion when the mats are connected.

Fick's law parameters are given in Table 2 for the original and patch concrete. Surface chloride concentration, C_o, was different for the patch and original concrete on the ocean facing side of the beam. The effective chloride diffusion coefficient, D, was also different for the patch and original concrete. The low chloride concentration on the beam surface (both ocean and landward sides) was the result of precipitation washing or runoff which leached Cl from the beam before it was sheltered for study. Over time this low value would have been balanced by much higher surface salt concentrations during drier periods that would lead to the profiles observed deeper in the concrete. In other words, the surface chloride concentration can vary considerably with time but the structure averages out these effects over time to give an effective C_o that correlates with the observed chloride profile.

In the US, D values range roughly from 0.6×10^{-8} to 7.5×10^{-8} cm^2/s, and C_o from 1.2 to 8.2 kg/m^3 (2.0 to 14 lb Cl/yd^3) [27]. D can vary with time as the concrete cures [33] or as the moisture content varies with environmental conditions, but does not appear to be greatly affected by transverse cracking of the concrete [27]. However, as with the surface chloride concentrations, the structure over time tends to average out these variations and responds with Fick's law parameters that are characteristic of the structure and its environment. Furthermore, Fick's law parameters obtained from structures, particularly older structures, are a valid basis for making predictions about that structures' performance [27]. Using the Fick's law values in Table 2, chloride profiles were generated for patch concrete in the Rocky Point Viaduct as a function of time, Fig. 10. Cover depth for shear stirrups on the beam vertical sides was 4.97, and 2.80 cm on the beam underside. The corresponding values for the square reinforcing bar were 6.75 and 4.96 cm. Fig. 10 shows corrosion would initiate first on the shear stirrups and that, given the severity of the environment, the concrete cover was inadequate to prevent corrosion damage. Using the values in Table 2, a chloride corrosion threshold for black iron bar of 0.74 kg Cl/m^3 (1.25 lb Cl/yd^3), and the cover depth for shear stirrups on the beam sides, the corrosion threshold would be reached in 3.1 yr for patch concrete on the west side, and 4.0 yr for the east side.

Corrosion propagation in concrete is a complex phenomena dependant primarily on moisture content and availability of oxygen. Once the corrosion threshold is reached, Stewart and Rosowsky [27] use a rate of 11–23 μm/yr (0.46–0.91 mpy) to model corrosion-induced deterioration of reinforced concrete structures. Roughly 25 μm (1 mil) corrosion loss has been considered sufficient to initiate cracking of concrete around reinforcing bar [32,34]. Considering these various factors, time-to-

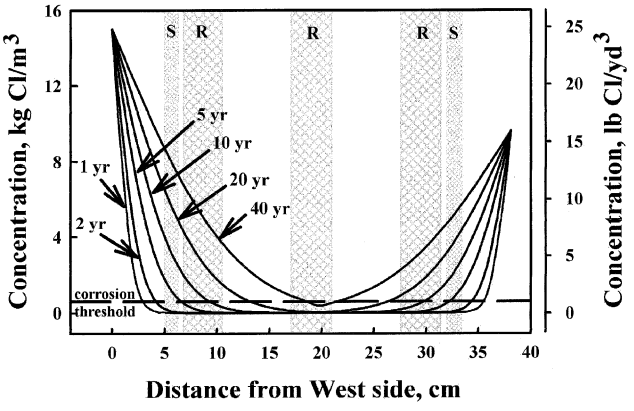

Fig. 10. Computed chloride profiles for patch concrete from the Rocky Point Viaduct (OR) showing the effect of time on profiles and cover depth on corrosion initiation. Position of reinforcing bar (R) and shear stirrups (S), and the chloride corrosion threshold (0.74 kg Cl/m^3) are shown.

corrosion cracking, once corrosion has been initiated, is estimated to be 3–4 yr [35] and 3–5 yr [34,36]. On this basis, the patch concrete delayed further damage to the structure by only 6–9 yr.

Similar computations for the original concrete yield times for corrosion initiation of 19.0 and 10.1 yr for the west and east sides of the beam. Add 3–5 yr for crack initiation [34–36], and corrosion damage should have been evident to bridge inspectors after 13–24 yr. In fact, these values include the time when corrosion damage was first observed (13 yr) and the time major repairs were made (15 yr).

One-foot thick transverse sections were cut from the beam containing the embedded reinforcing bar for a study of chloride migration under ICCP. ICCP was conducted at an accelerated rate so that the effects of 15 yr service could be observed in 1 yr. The thermal-sprayed zinc anode current density was 22 mA/m^2 (2.0 mA/ft^2) and cathode current density was 32 mA/m^2 (3.0 mA/ft^2). The resulting chloride profiles for the patch concrete are given in Fig. 9. The profiles for 0.5 and 1.0 yr ICCP were taken at different locations with respect to the reinforcing bar, leading to the 1.0 yr profile being slightly higher than the 0.5 yr profile on the west side of the beam.

Comparing the 0.5 yr profile with the "as-received" profile shows there was a net loss of chloride from the beam. The difference between the two curves was integrated from the beam centerline to the outer surface to compute the amount of chloride extracted. The value was 0.34 kg Cl/m^2 through the west vertical face and 0.04 kg Cl/m^2 through the east face. This was confirmed visually by salt encrusting the zinc anode on each face. One-dimensional finite-element analysis of chloride migration under superimposed concentration and potential gradients [37] reproduced the flattened profile seen in Fig. 9 between the square reinforcing bar (R) and the West side of the beam after 0.5 yr ICCP. The analysis predicted little change in chloride ion concentration below the depth of the outer square reinforcing bar. It also predicted little additional change in the profile for additional ICCP without washing of the anode surface by precipitation to remove surface chloride buildup.

Thus, severe environment and insufficient cover over shear stirrups were responsible for the early corrosion damage of the Rocky Point Viaduct requiring repair in 1969. Visual inspection and half-cell potential surveys supported this finding. The repair delayed further corrosion damage by no more than 6–9 yr and led to replacement of the Viaduct after only 40 yr service. Chloride migration studies on beam sections showed that ICCP can yield three benefits: (1) it prevents further corrosion damage to the steel reinforcing bar; (2) it can reduce the chloride concentration in concrete surrounding the reinforcing bar; and, presumably, (3) it can restore protective alkaline conditions at the bar–concrete interface.

4.2. Brush Creek Bridge (Oregon, USA)

The Brush Creek Bridge (1954–1998), a three-span, 244 m (800 ft) long, reinforced concrete deck girder bridge for US Route 101on the southern Oregon coast, just 9 km (5.6 miles) south of the Rocky Point Viaduct, was replaced in 1998 for the same reasons the Rocky Point Viaduct was replaced, severe corrosion-related structural damage. The microclimate was not as severe as that of the Rocky Point Viaduct. The bridge was less exposed, being 244 m (800 ft) from the ocean and at an elevation of 16 m (55 ft). However, delivery of salt to the bridge from salt spray and salt fogs was greatly increased by the local terrain which accelerated onshore winds.

Much of the concrete covering the deck underside spalled off, exposing the lower mat of reinforcing bar and greatly accelerating corrosion. Similarly, cover concrete spalled from the bottom of many of the beams, exposing the reinforcing bar and shear stirrups to further section loss. Some of the shear stirrups were rusted completely through. Damage was greatest along the leading edge of the beams nearest the ocean which collected salt spray that drained from the beam face.

Three 6 m (20 ft) beams (A2, A3, and A4) from the bridge were preserved for detailed evaluation of failure causes. One part of this evaluation was to identify significant structural, chemical, and environmental factors that contributed to the failure. The load–deflection curve for beam A4 was measured and showed a 24% loss in strength when compared to its design capacity. The failure mode was plastic deformation of the longitudinal reinforcement.

Chloride ion depth profiles were measured for the beams, the diaphragms, and the deck. Fick's law parameters for these profiles are summarized in Table 2. Surface concentration, C_o, varied widely with location on the bridge, indicating strong local interaction between the processes for salt delivery, wind patterns, washing by precipitation, fog, sheltering, and orientation. The effective chloride diffusion coefficient, D, tended to be higher on the ocean facing side of the beams and diaphragms. Like the Rocky Point Viaduct profiles, the results were not symmetrical between the vertical faces of the beams and diaphragms, reflecting the local environment of the beam and the condition of the beam surface.

Deck chloride profiles are shown in Fig. 11 along with the position of the upper and lower mats of reinforcing bar. Salt deposited to the deck top apparently was removed in precipitation runoff. Most chloride in

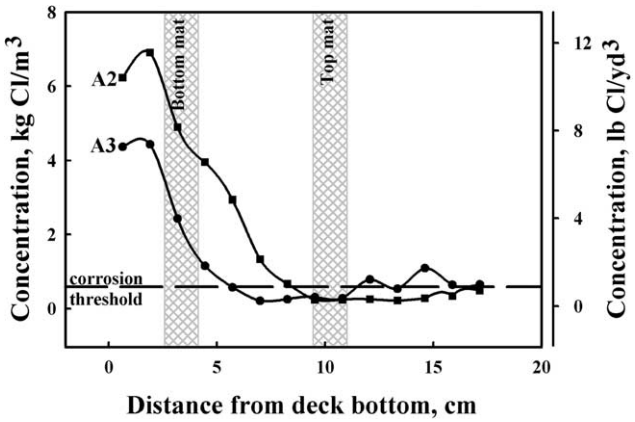

Fig. 11. Chloride profiles for 44 yr old deck attached to beams A2 and A3 from the Brush Creek Bridge (OR). Position of top and bottom reinforcing bar mats, and the chloride corrosion threshold (0.74 kg Cl/m^3) are shown.

the deck was concentrated near the bottom of the deck in a typical diffusion profile, with concentrations exceeding 6 kg/m^3(10 lb Cl/yd^3) at the bottom surface. Salt was delivered to this surface in salt spray and salt aerosols, concentrated in dew and moisture from fog, and had little chance for removal in precipitation runoff. Chloride concentrations at the top mat were below the chloride corrosion threshold; those at the lower mat were well above the threshold, providing an opportunity for macro-cell corrosion if the mats were connected and electrically continuous.

Using data in Table 2, the chloride threshold for black iron bar of 0.74 kg Cl/m^3(1.25 lb Cl/yd^3), and minimum measured cover depths for the lower reinforcing bar mat, 2.55 cm, the chloride threshold would have been reached for beam A2 in 3.7 yr, and for beam A3 in 9.5 yr. Add 3 to 5 yr for crack initiation [34–36] and visible damage to the concrete on the deck underside would have begun 7–14 yr after construction. Severe environment, inadequate cover depth, and the potential for macro-cell corrosion help explain the severe corrosion damage often observed on the underside of Oregon's coastal bridge decks and beams.

5. Stainless steel applications in new bridges

The weak link in reinforced concrete bridges is the susceptibility of the reinforcing bar to corrosion in high-chloride environments. Bare or epoxy-coated black iron bar is almost exclusively used as the reinforcement in these structures. Oregon DOT has decided the 10 to 20 yr benefit that may be realized from using epoxy-coated reinforcing bar, the hidden inspection, maintenance and repair costs associated, and the interference epoxy-coated bar poses to possible application of cathodic protection late in a structures life, does not warrant use of epoxy-coated bar in new bridge construction in the highly corrosive environment of the Oregon coast. Oregon's goal is to double or triple the life of the coastal bridges, to build bridges with a 120+ yr service life. This is not something that can economically be done with black bar or epoxy-coated bar.

In a broad sense, Oregon's goal can be achieved in three ways (here Fig. 10 is a useful reference). First, new grades of concrete, e.g., microsilica concrete (silica-fume concrete), with low effective chloride ion diffusion coefficients greatly retard salt transport into the concrete, steepening the chloride profile in the cover concrete, and extending substantially the time for chloride to reach the reinforcing bar. Oregon DOT presently specifies the use of microsilica concrete (4% microsilica maximum plus fly ash) in new coastal bridge construction. The minimum specified concrete cover is 38 mm (1.5 in.), a typical cover value is 51 mm (2 in.) and, in particularly harsh environments, 76 mm (3 in.) cover is specified. These cover specifications apply to all reinforcement, including shear stirrups, deck undersides and the bottom of beams.

A second way is to raise the chloride corrosion threshold of the reinforcing bar. While black iron bar and epoxy-coated black iron bar have a chloride threshold of 0.74 kg Cl/m^3 (1.25 lb Cl/yd^3), Type 304 stainless steel has a chloride threshold, in the absence of connections to black iron bar, of about 11 kg Cl/m^3 (19 lb Cl/yd^3) and Type 316 stainless a threshold of about 18 kg Cl/m^3(31 lb Cl/yd^3) [32]. Oregon DOT and others [38–40] have looked at these and other possible stainless bar compositions, including Nitronic 50 and duplex alloy 2205. An advantage of stainless steels for Oregon is that their chloride threshold exceeds the surface chloride concentrations observed on bridges in even harsh environments, Table 2. As a consequence, there should be essentially no corrosion of stainless reinforcing bar in Oregon's coastal bridges.

A third way is to lower the corrosion rate of the reinforcing bar. Black iron bar can corrode in chloride contaminated concrete at rates of 11–23 μm/yr (0.46–0.91 mpy) [27]. In contrast, stainless steels corrode at rates several orders of magnitude less, i.e., 0.05 μm/yr (0.002 mpy) [32]. Thus, once corrosion has initiated, stainless steel reinforcing bar would take far longer to build up sufficient corrosion products on their surface to cause cracking of the concrete.

While long-term benefits and problems from using stainless steel reinforcing bar in coastal bridge construction will not be known with certainty for generations, there are some examples that suggest the choice is sound when the goal is 120+ yr bridges. One such example is the Port of Progreso Pier in Yucatan, Mexico, built using Type 304 stainless reinforcing bar. It has been

Table 3
Materials costs for recent coastal bridge projects in Oregon using stainless steel reinforcing bar in corrosion critical areas and black iron bar

Project	Brush Creek	Smith River	Haynes Inlet
Year completed	1998	1999	2003
Stainless steel bar			
Uses	Deck, beams	Precast, prestressed girders[a]	Deck, beams
Alloy	316N	316N	316LN
Yield strength, MPa (ksi)	414 (60)	414 (60)	517 (75)
Unit price, $/kg ($/lb)	$7.88($3.58)	$262.47/girder-meter	$5.02($2.28)
Quantity, kg	42,270	2713 girder-meters	320,000
Total stainless cost[b]	$333,660	$712,080	$1,610,000
Equivalent black iron bar cost[b]	$107,790	Not available	$486,400
Black iron bar			
Unit price, $/kg ($/lb)	$2.55($1.16)	Not available	$1.52($0.69)
Quantity, kg	69,550	Not available	600,000
Total black iron bar cost[b]	$187,020	$390,900	$900,000
Project summary			
Total project cost[b]	$2,259,380	$8,565,080	$11,055,400
Stainless cost as % of project cost	14.8%	8.3%	14.5%
Stainless cost premium over black iron bar as % of project cost	10.0%	Not available	10.2%

[a] Reinforcing bar cast in girders.
[b] 1999 US dollars.

in service for over 60 yr in a hot, humid, and salty environment and has required virtually no maintenance [41].

Austenitic and duplex stainless steels appear to offer an acceptable combination of corrosion resistance, mechanical properties (yield strength), availability, and cost for coastal bridge applications. Oregon DOT now specifies solid (as opposed to clad) austenitic and duplex stainless steel reinforcing bar for new bridge construction on the Oregon coast. Black iron bar may be used in compressive members, in which case the stainless steel and black iron bar are electrically isolated from each other. The specification for stainless steel is based on yield strength, corrosion threshold, and corrosion rate. It is an "allowable" specification in that it allows a contractor to choose 316 LN, duplex 2205 alloy, or Nitronic 50. Oregon DOT has worked with the Federal Highway Administration to ensure that FHWA could support both the concept of doubling bridge service life through the use of stainless steel reinforcing bar and the format of the Oregon DOT "allowable" specification for use with Federal aid funding.

Oregon DOT has completed two bridge projects using stainless steel reinforcing bar and a third is under construction, Table 3. The latter project takes advantage of the ability of mills to work the steel to produce a higher yield strength so that less steel is required. In the next 6 yr, two additional bridge replacement projects will use stainless steel reinforcement in corrosion critical areas. Stainless steel bar is used in deck, beams, and precast girders. As noted earlier, bare black iron bar is used in compression members, i.e., columns and arches. While stainless steel and black iron bar are always electrically isolated from each other, each type of bar are electrically continuous so that cathodic protection can be used if required at a later date, a reasonable precaution when applying new technology. Microsilica concrete was employed throughout the structures, including the deck where its abrasion resistance is an advantage.

Costs for the stainless steel and black iron bar used in these projects is given in Table 3. The total steel prices are simply the unit price times the quantity. The cost of black iron bar equivalent to the stainless steel used in corrosion critical areas is given as a separate entry. While stainless steel bar costs a factor of three or more than black iron bar, use of stainless steel in the projects raised total project costs only 10% compared to the equivalent quantity of black iron bar, Table 3. At a minimum, it is anticipated the use of stainless steel will double bridge life while cutting cumulative costs, relative to conventional black iron bar, by 50% over the life of the bridges.

6. Conclusions

6.1. Planar cathodic protection anodes

Planar anodes are the most effective configuration for reducing electrolyte (concrete) resistance and improving current distribution to reinforcing bar in concrete bridges. Thermal-sprayed anodes and foil anodes with a conductive adhesive can achieve these objectives. Thermal-sprayed zinc anodes may have a service life ex-

ceeding 25 yr at the Oregon DOT bridge CP current density of 2.2 mA/m^2 based on the effects of electrochemical age on anode bond strength. A resistive layer develops at the anode–concrete interface with increasing electrochemical age, thereby increasing anode polarization. In ICCP systems this is reflected in a higher circuit resistance; in GCP systems it results in lower current output. Periodic wetting of the anode by rain, fog, and dew is an important factor in reducing anode polarization. Bridge structure wetting and drying cycles are reflected in the operation of thermal-sprayed zinc anodes.

As an alternative to thermal-sprayed zinc anodes, catalyzed thermal-sprayed titanium anodes under ICCP service develop no significant anode polarization with electrochemical age. They perform well in both low and high humidity environments, and exhibit stable long-term performance. The catalyst is located at the anode–concrete interface and appears fairly resistant to leaching by precipitation washing. In GCP service, zinc-hydrogel anodes produce a stable protection current sufficient to protect reinforcing bar from corrosion. There was practically no effect of changing environmental conditions (moisture) on current production and no evidence of aging effects in an Oregon DOT field trial. The hydrogel anodes are readily topcoated to provide visual compatibility with bridge surroundings.

6.2. Anode chemical treatments – humectants

Moisture at the thermal-sprayed zinc anode–concrete interface greatly reduces the resistance of the growing zinc mineral layer produced by aging. Humectants (moisture attractants), such as lithium nitrate and lithium bromide, show promise as a treatment for thermal-sprayed zinc anodes by increasing the moisture at this interface. Lithium bromide is the more powerful humectant in GCP applications and results in higher current output from the zinc anode. Humectants can also reduce the circuit resistance of ICCP anodes electrochemically aged prior to humectant application. However, the best time to apply humectants is immediately after applying the thermal-sprayed zinc anode, since humectants improve the performance of both new and previously aged zinc anodes and needed site preparation is already in place for new anodes.

6.3. Bridge evaluation methodology and construction practices

Forensic analysis of failed coastal bridge elements identified critical factors leading to their failure, effective methodology for identifying corrosion-related problems, and construction practice changes that would prevent similar problems in new structures. Chloride profiling is one of the more powerful and economical tools available for assessing potential corrosion problems in a structure. When done at sufficient resolution and with adequate care to establish good estimates of the effective diffusion coefficient, D, and surface chloride concentration, C_o, chloride profiles computed using Fick's Law can be analyzed relative to the location of reinforcing bar to identify potential corrosion problems and make reasonable estimates of time-to-cracking. When good estimates of D and C_o, are available, future chloride monitoring of concrete can be limited and infrequent. All other factors being equal, D is a measure of concrete durability; C_o is a measure of microclimate corrosivity. C_o is a function of structure location relative to water and local land forms, sheltering, washing by precipitation, wind patterns through the structure, local microclimates, and porosity of the concrete. As a consequence, C_o varies throughout the structure and leads to a varied pattern of corrosion damage. Inadequate cover depth, particularly over shear stirrups and the bottom mat in bridge decks, coupled with a harsh environment were the primary causes of corrosion-related structural failures.

6.4. Stainless steel applications in new bridges

Austenitic and duplex stainless steels provide an acceptable combination of corrosion resistance, yield strength, availability, and cost for reinforcing bar in coastal bridge construction. Current Oregon DOT specifications call for the use of stainless steel bar in corrosion critical areas, such as deck, beams and precast prestressed girders, in future coastal bridge construction. Black iron bar may be used in compressive members. Stainless steel and black iron bar are required to be electrically isolated from each other. Specifications also call for the use of microsilica concrete, with the microsilica component at 4% maximum. Two coastal bridges have been constructed using austenitic stainless steel reinforcing bar and three additional bridge replacement projects are in progress or planned. Stainless steel bar adds a premium of only 10% to total project costs, compared to black iron bar. However, it is expected to yield a 120+ yr bridge service life due to a much higher corrosion threshold in chloride-contaminated concrete and a substantially lower corrosion rate while reducing cumulative bridge life costs by 50%.

References

[1] Burke P. Status of the nation's bridges. Mater Performance 1994;33(6):48.
[2] Deterioration of Oregon Coast Highway Bridges. Oregon Department of Transportation: Salem, OR; 1984.

[3] Mudd CJ, Mussinelli GL, Tettamanti M, Pediferri P. Cathodic protection of steel in concrete. Mater Performance 1988;27(9): 18–24.
[4] Jackson D. Focus. Washington, DC: US Department of Transportation, Federal Highway Administration; 1997. p. 5.
[5] Carello RA, Parks DM, Apostolos JA. Development, testing and field application of metallized cathodic protection coatings on reinforced concrete substructures, FHWA/CA/TL-89/04. California Department of Transportation; 1989.
[6] Holcomb GR, Cryer CB. Cost of impressed current cathodic protection for coastal Oregon bridges. Mater Performance 1998;37(7):22–6.
[7] McGill GE, Cramer SD, Covino Jr BS, Bullard SJ, Holcomb GR, Collins WK, Govier RD, Wilson RD. Field application of an arc-sprayed titanium anode for cathodic protection of reinforcing steel in concrete, FHWA-OR-RD-99-13. Washington, DC: US Department of Transportation, Federal Highway Administration; 1999.
[8] Cramer SD, Covino Jr. BS, Holcomb GR, Bullard SJ, Collins WK, Govier RD, Wilson RD, Laylor HM. Concrete bridges thermal-sprayed titanium anode for cathodic protection of reinforced. J Thermal Spray Technol 1999;8(1):133–45.
[9] Bullard SJ, Covino BS Jr, Cramer SD, Holcomb GR, Russell JH, Cryer CB, Laylor HM. Alternative consumable anodes for cathodic protection of reinforced concrete bridges. CORROSION/99, Paper No.99544. Houston TX: NACE International; 1999.
[10] Bullard SJ, Covino BS Jr, Cramer SD, Holcomb GR, Russell JH, Bennett JE, Cryer CB, Laylor HM. Alternative consumable anodes for cathodic protection of reinforced concrete bridges. Paper No. 28. In: Proceedings of the 14th International Corrosion Congress, Kelvin, South Africa: CorrISA; 1999.
[11] Rogers F, Thermion, Inc. Personal communication to SD Cramer; Albany Research Center, US Department of Energy, Albany OR, May 17, 2000.
[12] Grauer R, Moreland PJ, Pini G. A literature review of the polarisation resistance constant values for the measurement of corrosion rate. Houston TX: NACE International; 1982.
[13] Holcomb GR, Bullard SJ, Covino BS Jr, Cramer SD, Cryer CB, McGill GE. Electrochemical aging of thermal-sprayed zinc anodes on concrete. In: Berndt CC, editor. Thermal spray: practical solutions for engineering problems. Metals Park, OH: ASM International; 1996. p. 185–92.
[14] Covino Jr. BS, Bullard SJ, Holcomb GR, Cramer SD, McGill GE, Cryer CB. Bond strength of electrochemically aged arc-spray coatings on concrete. Corrosion 1997;53(5):399–411.
[15] Bullard SJ, Cramer SD, Covino Jr BS, Holcomb GR, McGill GE, Reis R. Thermal-sprayed anodes for cathodic protection of reinforced concrete bridges. In: GjØrv OE, Sakai, K, Banthia N editors. Concrete under severe conditions 2: environment and loading, CONSEC '98, London: E&FNSpon; 1998. p. 959–68.
[16] Bullard SJ, Covino BS Jr, Holcomb GR, Cramer SD, McGill GE. Bond strength of thermal-sprayed zinc on concrete during early stages of electrochemical aging. CORROSION/97. Paper No. 97232; March 1997.
[17] Bullard SJ, Cramer SD, Covino Jr BS, Holcomb GR, McGill GE, Reis R. Thermal-sprayed zinc anodes – laboratory and field studies. In: Proceedings of SSPC97-09 Expanding Coatings Knowledge Worldwide, Steel Structures Paint Council; November 1997. p. 309–19.
[18] Types of Portland Cement and Increase in Strength of Concrete With Age. In: Lynch CT, editor. Practical handbook of materials science. Boca Raton, FL: CRC Press; 1989. p. 190.
[19] Bennett J, Firlotte C. A zinc-hydrogel system for cathodic protection of reinforced concrete structures. Paper No. 96316, CORROSION/96. Houston TX: NACE International; 1996.
[20] Bennett JE, Schue TJ. Galvanic Cathodic protection of reinforced concrete bridge members using sacrificial anodes attached by conductive adhesives. FHWA-RD-99-112. Washington, DC: US Department of Transportation, Federal Highway Administration; September 1999.
[21] Kessler RJ, Powers RG, Lasa IR. Cathodic protection using zinc sheet anodes and an ion conductive gel adhesive. Paper No. 97234, CORROSION/97. Houston TX: NACE International; 1997.
[22] Bennett J. Chemical enhancement of metallized zinc anode performance. Paper No. 98640, CORROSION/98. Houston TX: NACE International; 1998.
[23] Covino Jr BS, Bullard SJ, Holcomb GR, Russell JH, Cramer SD, Bennett JE, Laylor HM. Chemical modification of thermal-sprayed zinc anodes for improved cathodic protection of reinforced concrete. Paper No. 33, In: Proceedings of the 14th International Corrosion Congress, Kelvin, South Africa: CorrISA; 1999.
[24] Holcomb GR, Covino BS Jr, Russell JH, Bullard SJ, Cramer SD, Collins WK, Bennett JE, Laylor HM. Humectant use in the cathodic protection of reinforced concrete. Paper No. 00812, CORROSION/2000. Houston TX: NACE International; 2000.
[25] Covino Jr. BS, Cramer SD, Holcomb GR, Bullard SJ, Laylor HM. Postmortem of a failed bridge. Concr Int 1999;21(2):39–45.
[26] Cramer SD, Covino BS Jr, Holcomb GR, Bullard SJ, Dahlin CM, Summers CA, Laylor HM, Soltesz SM. Evaluation of rocky point viaduct concrete beam. FHWA-OR-RD-00-18. Washington, DC: US Department of Transportation, Federal Highway Administration; June 2000.
[27] Stewart MG, Rosowsky DV. Structural safety and serviceability of concrete bridges subject to corrosion. J Infrastructure Syst 1998;4(4):146–55.
[28] Broomfield JP. Corrosion of steel in concrete. E&FN Spon: New York; 1997. p. 23–4.
[29] Cady PD, Weyers RE. Chloride penetration and deterioration of concrete bridge decks. Cem Concr Aggregates 1983;5(2):81–7.
[30] Hausmann DA. Steel corrosion in concrete: how does it occur. Mater Protection 1967;6(11):19–23.
[31] Mehta EK. Concrete in the marine environment. UK: Elsevier Applied Science Barking; 1991.
[32] McDonald DB, Pfeifer DW, Sherman MR. Corrosion evaluation of epoxy-coated, metallic-clad and solid metallic reinforcing bars in concrete. FHWA-RD-98-153. Washington, DC: US Department of Transportation, Federal Highway Administration: December; 1998.
[33] Bentz DP, Clifton JR, Snyder KA. Predicting service life of chloride-exposed steel-reinforced concrete. Concr Int 1996;18(12):42–7.
[34] McDonald DB, Pfeifer DW, Blake GT. The corrosion performance of inorganic- ceramic-, and metallic-clad reinforcing bars in accelerated screening tests. FHWA-RD-96-085. Washington, DC: US Department of Transportation, Federal Highway Administration; December, 1996.
[35] Sagues AA. Corrosion of epoxy coated rebar in florida bridges. Final report to Florida Department of Transportation, WPI No. 0510603. Tampa FL: University of South Florida; 1994.
[36] Liu, Y, Weyers, RE. Modeling the time-to-corrosion cracking in chloride contaminated reinforced concrete structures. Am Concr Inst Mater J;1998:675–81.
[37] Jost W. Diffusion in solids, liquids, and gases. NY: Academic Press; 1960. p. 47.
[38] McGurn JF. Stainless steel reinforcing bars in concrete. In: Proceedings of the International Conference on Corrosion and Rehabilitation of Reinforced Concrete Structures. Washington, DC: US Department of Transportation, Federal Highway Administration; December 1998.

[39] Rasheeduzzafar, Dakhil FH, Brader MA, Khan MM. Performance of corrosion resisting steels in chloride-bearing concrete. ACI Mater J 1992;89(5):439–48.
[40] Pastore T, Pedeferri B. Corrosion behavior of a duplex stainless steel in chloride contaminated concrete. In: Proceedings of the International Conference on Stainless Steels; Chiba: ISIJ; 1991. p. 351–8.
[41] Ramboll Consulting Engineers. Pier in progreso Mexico inspection Report – evaluation of stainless steel reinforcement. Arminox, Viborg Denmark; March; 1999.